Chapter 9
Beam Deposition Processes

9.1 Introduction

Beam deposition (BD) processes enable the creation of parts by melting and deposition of material from powder or wire feedstock. Although this basic approach can work for polymers, ceramics, and metal matrix composites, it is predominantly used for metal powders. Thus, this technology is often referred to as "metal deposition" technology. To avoid limiting the readers' understanding to just metal build materials, however, we will refer to this category of processes as beam deposition processes.

BD processes use some form of energy focused into a narrow region (a beam), which is used to heat a material that is being deposited. Unlike the powder bed fusion techniques discussed in Chap. 5, BD processes are NOT used to melt a material that is pre-laid in a powder bed but are used to *melt materials as they are being deposited*.

BD processes use a focused heat source (such as a laser, electron beam or plasma arc) to melt the feedstock material and build up 3-dimensional objects in a manner similar to the extrusion-based processes from Chap. 6. Each pass of the BD head creates a track of solidified material, and adjacent lines of material make up layers. Complex 3-dimensional geometry requires either support material or a multiaxis deposition head. A schematic representation of a BD process using powder feedstock material and laser is shown in Fig. 9.1.

Most commercialized BD processes enable complete melting of powders using a focused high-power laser beam as the heat source. Research variants include using an electron beam or plasma source in place of the laser beam or the use of a thin metal wire instead of powder as the build material. In many ways, BD techniques can be used in an identical manner to laser cladding and plasma welding machines. For the purposes of this chapter, however, BD machines are considered as those which are designed to create depositions of complex 3D shapes directly from CAD files, rather than the traditional welding and cladding technologies, which were designed for repair, joining, or to apply coatings and do not typically use 3D CAD data as an input format.

I. Gibson, D.W. Rosen, and B. Stucker, *Additive Manufacturing Technologies*,
DOI 10.1007/978-1-4419-1120-9_9,

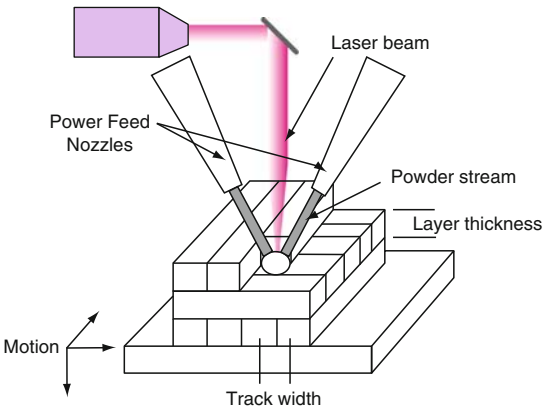

Fig. 9.1 Schematic of a typical beam deposition process

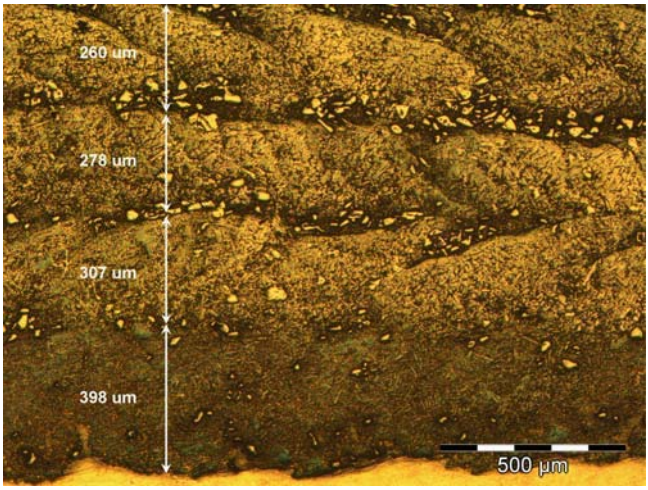

Fig. 9.2 LENS-deposited Ti/TiC metal matrix composite structure (4 layers on top of a Ti substrate)

A number of organizations have developed BD machines using lasers and powder feeders. These machines have been referred to as Laser Engineered Net Shaping (LENS) [1], Directed Light Fabrication (DLF) [2], Direct Metal Deposition (DMD), 3D Laser Cladding, Laser Generation, Laser-Based Metal Deposition (LBMD), Laser Freeform Fabrication (LFF), Laser Direct Casting, LaserCast [3], Laser Consolidation, LasForm and others. Although the general approach is the same, differences between these machines commonly include changes in laser power, laser spot size, laser type, powder delivery method, inert gas delivery method, feedback control scheme, and/or the type of motion control utilized. Because these processes all involve deposition, melting and solidification of powdered material using a traveling melt pool, the resulting parts attain a high density during the build process (although the surface often has porosity due to adhered partially molten particles). The microstructure of parts made from BD processes

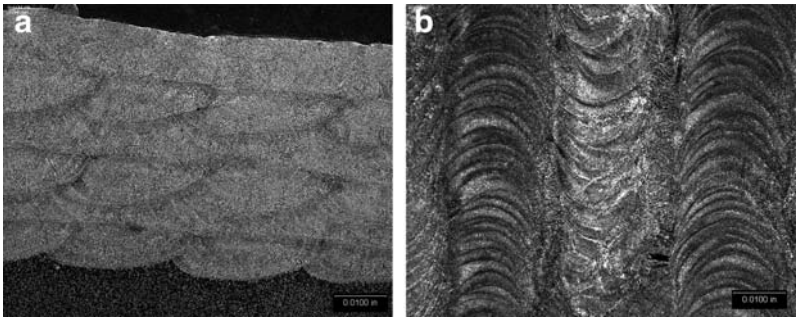

Fig. 9.3 CoCrMo deposit on CoCrMo: (**a**) side view (every other layer is deposited perpendicular to the previous layer using a 0,90,0 pattern); and (**b**) top view of deposit

(Figs. 9.2 and 9.3) are similar to powder bed fusion processes (*see* Fig. 5.14), wherein each pass of the laser or heat source creates a track of rapidly solidified material.

As can be seen from Figs. 9.2 and 9.3, the microstructure of a BD part can be different between layers and even within layers. In the Ti/TiC deposit shown in Fig. 9.2, the larger particles present in the microstructure are unmelted carbides. The presence of fewer unmelted carbides in a particular region is due to a higher overall heat input for that region of the melt pool. By changing process parameters, it is possible to create fewer or more unmelted carbides within a layer, and by increasing laser power, for instance, a greater amount of the previously deposited layer (or substrate for the first layer) will be re-melted. By comparing the thickness of the last-deposited layer with the first or second a previously-deposited layer (such as in Fig. 9.3a), an estimate of the proportion of a layer that is remelted during subsequent deposition can be made. Each of these issues is discussed in the following section.

9.2 General Beam Deposition Process Description

As the most common type of beam deposition system is powder-based laser deposition system optimized for metals, we will use a typical laser-based metal deposition (LBMD) process as the paradigm process against which other processes will be compared. In LBMD, a "deposition head" is utilized to deposit material onto the substrate. A deposition head is typically an integrated collection of laser optics, powder nozzle(s), inert gas tubing, and in some cases, sensors. The substrate can be either a flat plate on which a new part will be fabricated or an existing part onto which additional geometry will be added. Deposition is controlled by relative differential motion between the substrate and deposition head. This differential motion is accomplished by moving the deposition head, by moving the substrate, or by a combination of substrate and deposition head motion. 3-axis systems, whereby the deposition occurs in a vertical manner, are typical. However, 4- or 5-axis systems using either rotary tables or robotic arms are also available.

The kinetic energy of powder particles being fed into the melt pool is greater than the effect of gravity on these powders during flight. As a result, nonvertical deposition is just as effective as vertical deposition. Multi-axis deposition head motion is therefore possible and, indeed quite useful. In particular, if the substrate is very large and/or heavy, it is easier to accurately control the motion of the deposition head than the substrate. Conversely, if the substrate is a simple flat plate, it is easier to move the substrate than the deposition head. Thus, depending on the geometries desired and whether new parts will be fabricated onto flat plates or new geometry will be added to existing parts, the optimum design of a LBMD apparatus will change.

In LBMD, the laser generates a small molten pool (typically 0.25–1 mm in diameter and 0.1–0.5 mm in depth) on the substrate as powder is injected into the pool. The powder is melted as it enters the pool and solidifies as the laser beam moves away. Under some conditions, the powder can be melted during flight and arrive at the substrate in a molten state; however, this is atypical and the normal procedure is to use process parameters that melt the substrate and powder as they enter the molten pool.

The typical small molten pool and relatively rapid traverse speed combine to produce very high cooling rates (typically 1,000–5,000°C/s) and large thermal gradients. Depending upon the material or alloy being deposited, these high cooling rates can produce unique solidification grain structures and/or nonequilibrium grain structures which are not possible using traditional processing. At lower cooling rates (when using higher beam powers or lower traverse speeds), the grain features grow and look more like cast grain structures.

The passing of the beam creates a thin track of solidified metal deposited on and welded to the layer below. A layer is generated by a number of consecutive overlapping tracks. The amount of track overlap is typically 25% of the track width (which results in re-melting of previously deposited material) and typical layer thicknesses employed are 0.25–0.5 mm. After each layer is formed, the deposition head moves away from the substrate by one layer thickness.

9.3 Material Delivery

BD processes can utilize both powder and wire feedstock material. Each has limitations and drawbacks with respect to each other.

9.3.1 Powder Feeding

Powder is the most versatile feedstock, and most metal and ceramic materials are readily available in powder form. However, not all powder is captured in the melt pool (e.g., less than 100% powder capture efficiency), so excess powder is utilized

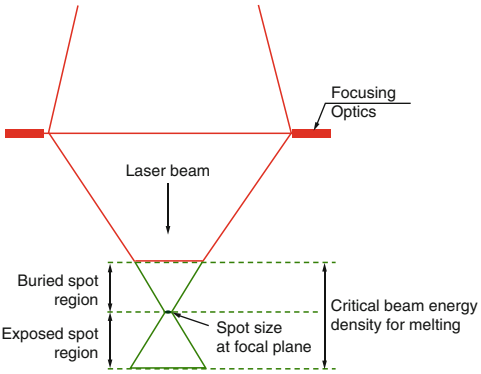

Fig. 9.4 Schematic illustrating laser optics and energy density terminology for beam deposition

and care must be taken to ensure this excess powder is recaptured in a clean state if recycling is desired.

Excess powder feeding, however, is not necessarily a negative attribute, as it makes BD processes geometrically flexible and forgiving. This is due to the fact that excess powder flow enables the melt pool size to dynamically change. As described below, BD processes using powder feeding can enable overlapping scan lines to be used without the swelling or overfeeding problems inherent in extrusion-based processes (discussed in Section 6.3).

In BD, the energy density of the beam must be above a critical amount to form a melt pool on the substrate. When a laser is focused to a small spot size, there is a region above and below the focal plane where the laser energy density is high enough to form a melt pool. This region is labeled in Fig. 9.4. If the substrate surface is either too far above or too far below the focal plane, no melt pool will form. Similarly, the melt pool will not grow to a height that moves the surface of the melt pool outside this region.

Within this critical beam energy density region, the height and volume of the deposit melt pool is dependent upon melt pool location with respect to the focal plane, scan rate, laser power, powder flow rate, and surface morphology. Thus, for a given set of parameters, the deposit height approaches the layer thickness offset value only after a number of layers of deposition. This is evident, for instance, in Fig. 9.2, where a constant layer thickness of 200 μm was used as the deposition head z-offset for each layer. The substrate was initially located within the buried spot region, but not far enough within it to achieve the desired thickness for the layers shown (i.e., the laser power, scan rate and powder flow settings caused the deposit to be thicker than the layer thickness specified). Thus, deposit thickness approached the layer thickness z-offset as the spot became effectively more "buried" during each subsequent layer addition. In Fig. 9.2, however, too few layers were deposited to reach the steady-state layer thickness value.

If the laser and scanning parameters settings used are inherently incapable of producing a deposit thickness at least as thick as the layer thickness z-offset value, subsequent layers will become thinner and thinner. Eventually, no deposit will

occur when scanning for the next layer starts outside the critical energy density region (i.e., when the substrate starts out below the exposed spot region, there is insufficient energy density to form a melt pool on the substrate).

In practice, when the first layer is formed on a substrate, the laser focal plane is typically buried below the surface of the substrate approximately 1 mm. In this way, a portion of the substrate material is melted and becomes a part of the melt pool. The first layer, in this case, will be made up of a mixture of melted substrate combined with material from the powder feeders, and the amount of material added to the surface for the first layer is dependent upon process parameters and focal plane location with respect to the substrate surface. If little mixing of the substrate and deposited material is desired, then the focal plane should be placed at or above the substrate surface to minimize melting of the substrate – resulting in a melt pool made up almost entirely of the powdered material. This may be desirable, for instance, when depositing a first layer of "material A" on top of "material B" that that might form "intermetallic AB" if mixed in a molten state. In order to suppress intermetallic formation, a sharp transition from A to B is typically required.

In summary, the first few layers may be thicker or thinner than the layer thickness set by the operator, depending upon the focal plane location with respect to the substrate surface and the process parameters chosen. As a result, the layer thickness converges to the steady-state layer thickness setting after several layers or, if improper parameters are utilized, the laser "walks away" from the substrate and deposition stops after a few layers.

The dynamic thickness benefits of powder feeding also help overcome the corrugated surface topology associated with BD. This corrugated topology can be seen in Fig. 9.3b and is a remnant of the set of parallel, deposited tracks (beads) of material which make up a layer. As in extrusion-based AM processes, in BD a subsequent layer is typically deposited in a different orientation than the previous layer. Common scan patterns from layer to layer are typically multiples of 30, 45 and 90 degrees (e.g. 0, 90, 0, 90. . .; 0, 90, 180, 270, 360. . .; 0, 45, 90. . .315, 360. . .; and 0, 30, 60. . .330, 360. . .). Layer orientations can also be randomized between layers at pre-set multiples. The main benefits of changing orientation from layer-to-layer are the elimination of preferential grain growth (which otherwise makes the properties anisotropic) and minimization of residual stresses.

Changing orientation between layers can be accomplished easily when using powders, as the presence of excess powder flow provides for dynamic leveling of the deposit thickness and melt pool at each region of the deposited layer. This means that powdered material feedstock allows the melt pool size to dynamically change to fill the bottoms of the corrugated texture without growing too thick at the top of each corrugation. This is not the case for wire feeding.

Powder is typically fed by first fluidizing a container of powder material (by bubbling up a gas through the powder and/or applying ultrasonic vibration) and then using a pressure drop to transfer the fluidized powder from the container to the laser head through tubing. Powder is focused at the substrate/laser interaction zone using either co-axial feeding, 4-nozzle feeding, or single nozzle feeding. In the case of co-axial feeding, the powder is introduced as a toroid surrounding the laser beam,

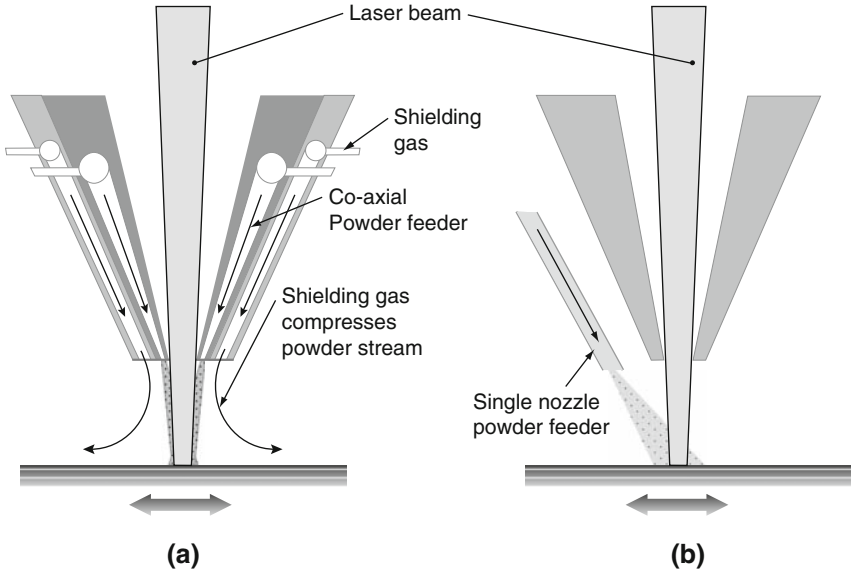

Fig. 9.5 Illustration of powder nozzle configurations: (**a**) co-axial nozzle feeding; and (**b**) single-nozzle feeding

which is focused to a small spot size using shielding gas flow, as illustrated in Fig. 9.5a. The two main benefits of co-axial feeding are that it enables a higher capture efficiency of powder, and the focusing shielding gas can protect the melt pool from oxidation when depositing in the presence of air. Single nozzle feeding involves a single nozzle pointed at the interaction zone between the laser and substrate. The main benefits of single nozzle feeding are the apparatus simplicity (and thus lower cost), a better powder capture efficiency than 4-nozzle feeding, and the ability to deposit material into tight locations (such as when adding material to the inside of a channel or tube). 4-nozzle feeding involves 4 separate nozzle heads equally spaced at 90 degree increments around the laser beam, focused to intersect at the melt pool. The main benefit of a 4-nozzle feeding system is that the flow characteristics of 4-nozzle feeding gives more consistency in build height for complex and arbitrary 3D geometries that involve combinations of thick and thin regions.

9.3.2 Wire Feeding

In the case of wire feeding, the volume of the deposit is always the volume of the wire that has been fed, and there is 100% feedstock capture efficiency. This is

effective for simple geometries, coating of surfaces, and/or deposits where porosity is acceptable. However, when complex, large, and/or fully dense parts are desired, geometry-related process parameters (such as hatch width, layer thickness, wire diameter, and wire feed rate) must be carefully controlled to achieve a proper deposit size and shape. Just as in extrusion-based processes, large deposits with geometric complexity must have porosity designed into them to remain geometrically accurate. For certain geometries, it is not possible to control the geometry-related process parameters accurately enough to achieve both high accuracy and low porosity with a wire feeder unless periodic subtractive processing (such as CNC machining) is done to reset the geometry to a known state. Thus, the selection of a wire feeding system versus a powder feeding system is best done after determining what type of deposit geometries are required and whether a subtractive milling system will be integrated with the additive deposition head.

9.4 BD Systems

One of the first commercialized BD processes, LENS, was developed by Sandia National Laboratories, USA, and commercialized by Optomec Design Company, USA. Optomec's "LENS 750" machine was launched in 1997. Subsequently, the company launched its "LENS 850" and "LENS 850-R" with larger build volume (460 × 460 × 1,070 mm) and dual laser head capability. Optomec's machines originally used an Nd-YAG laser, but more recent machines, such as their MR-7 research system, utilize fiber lasers.

Fig. 9.6 Optomec LENS 750 system (courtesy Optomec)

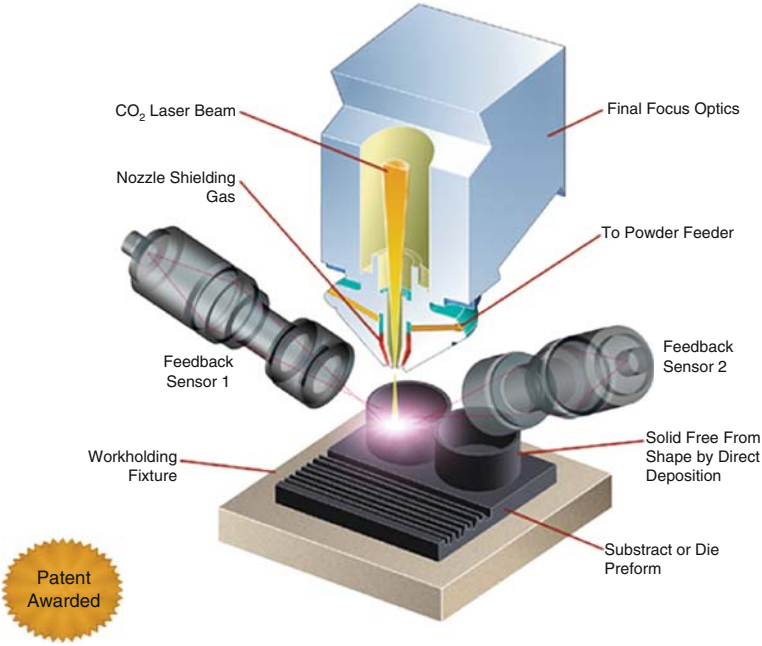

Fig. 9.7 POM, DMD machine schematic (courtesy POM)

LENS machines process materials in an enclosed inert gas chamber (*see* Fig. 9.6). An oxygen removal, gas recirculation system is used to keep the oxygen concentration in the gas (typically argon) near or below 10 ppm oxygen. The inert gas chamber, laser type, and 4-nozzle feeder design utilized by Optomec make their LENS machines some of the most flexible platforms for BD, as many materials can be effectively processed with this combination of laser type and atmospheric conditions. Most LENS machines are 3-axis and do not use closed-loop feedback control, however Optomec now offers a 5-axis "laser wrist" system that can enable deposition from any orientation, and systems for monitoring build height and melt pool area can be used to dynamically change process parameters to maintain constant deposit characteristics.

POM, USA, is another company building LBMD machines. Their DMD machines with 5-axis, co-axial powder feed capability can build parts without support structures using a shielding gas approach. A key feature of POM machines has always been the integrated closed-loop control system (*see* Fig. 9.7). Three CCD cameras are used as an optical feedback system, which continuously monitor in real time the size of the weld pool. The feedback control system adjusts process variables such as powder flow rate, deposition velocity and laser power to maintain deposit conditions. A CO_2 laser system with variable laser spot size enables fast builds and/or better feature definition, depending upon the spot size used. The use of CO_2 lasers has the benefit of being an economical, high-powered heat source, but the absorptivity of most materials is much less at CO_2 laser wavelengths than for

Fig. 9.8 AeroMet System (courtesy MTS Systems Corp.)

Nd-YAG or fiber lasers (as discussed in Chap. 5 and shown in Fig. 5.10). In order to compensate for this lower absorptivity, a larger amount of laser energy is applied, resulting in a larger heat affected zone and overall heat input into the substrate when compared with a LENS machine.

Another company which was involved early in the development of BD machines was AeroMet Inc., USA – until the division was closed in 2005. The AeroMet machine was specifically developed for producing large aerospace "rib-on-plate" components using prealloyed titanium powders and an 18 kW CO_2 laser (*see* Fig. 9.8). Although they were able to demonstrate the effectiveness of building rib-on-plate structures cost-effectively, the division was not sustainable financially and was closed. The characteristics of using such a high-powered laser are that large deposits can be made quite quickly, but at the cost of geometric precision and a much larger heat affected zone.

As BD technologies become accepted in the aerospace industry, a similar system will likely become commercialized again. The benefits behind adding features to simple shapes to form aerospace and other structures with an otherwise poor "buy-to-fly" ratio makes sense. The term buy-to-fly refers to the amount of wrought material that is purchased as a block that is required to form a complex part. In many cases, 80% or more of the material is machined away to provide a stiff, lightweight frame for aerospace structures. By building ribs onto flat plates using BD, the amount of waste material can be reduced significantly. This has both significant cost and environmental benefits. This is also true for other geometries where small features protrude from a large object, thus requiring a significant waste of material when machined from a block. This benefit is illustrated in the electronics housing deposited using LENS on the hemispherical plate shown in Fig. 9.9.

Another example of BD is the laser consolidation process from Accufusion, Canada. Laser consolidation was developed by the Canadian National Research

Fig. 9.9 Electronics Housing in 316SS. (Courtesy Optomec and Sandia National Laboratories)

Council's Integrated Manufacturing Technologies Institute. The key features of this process are the small spot-size laser, accurate motion control, and single-nozzle powder feeding. This enables the creation of small parts with much better accuracy and surface finish than other BD processes, but with the drawback of a significantly lower deposition rate.

Controlled Metal Buildup (CMB) is a hybrid metal deposition process developed by the Fraunhofer Institute for Production Technology, Germany. It illustrates an integrated additive and subtractive manufacturing approach that a number of research organizations are experimenting with around the globe. In CMB, a diode laser beam is used and the build material is introduced in the form of a wire. After depositing a layer, it is shaped to the corresponding slice contour by a high-speed milling cutter. The use of milling after each deposited layer eliminates the geometric drawbacks of a wire feeder and enables highly accurate parts to be built. The process has been applied primarily to weld repairs and modifications to tools and dies.

Electron Beam Freeform Fabrication (EBF^3) was developed by NASA Langley, USA, as a way to fabricate and/or repair aerospace structures both terrestrially and in future space-based systems. Using an electron beam as a thermal source and a wire feeder, EBF^3 is capable of rapid deposition under high current flows, or more accurate depositions using slower deposition rates. The primary considerations which led to the development of EBF^3 for space-based applications include: electron beams are much more efficient at converting electrical energy into a beam than most lasers, which conserves scarce electrical resources; electron beams work effectively in a vacuum but not in the presence of inert gases and thus are well suited for the space environment; and powders are inherently difficult to contain safely in low-gravity environments and thus wire feeding is preferred.

Several research groups have investigated the use of welding and/or plasma-based technologies as a heat source for BD. One such group at Southern Methodist University, USA, has utilized gas metal arc welding combined with 4-½ axis milling to produce 3-dimensional structures. Similar work has also been demonstrated by the Korea Institute of Science and Technology, which demonstrated combined CO_2 arc welding and 5-axis milling for part production. These approaches are viable and useful as lower-cost alternatives to laser and electron

beam approaches, however the typically larger heat-affected-zone and other process control issues have kept this approach from widespread commercialization.

9.5 Process Parameters

Unlike SLA, FDM and SLS, which come pre-programmed with optimized process parameters for materials sold by the machine vendors, BD machines are sold as flexible platforms; and thus BD users must identify the correct process parameters for their application and material. Optimum process parameters are material dependent and application/geometry dependent. Important process parameters include track scan spacing, powder feed rate, laser traverse speed, laser power, and laser spot size. Powder feed rate, laser power and traverse speed are all interrelated; for instance, an increase in feed rate has a similar effect to lowering the laser power. Likewise, increasing laser power or powder feed rate and decreasing traverse speed all increase deposit thickness. From an energy standpoint, as the scan speed is increased, the input laser energy decreases because of the shorter laser dwell time, resulting in a smaller melt pool on the substrate and more rapid cooling.

Scan pattern also plays an important role in part quality. As mentioned previously, it may be desirable to change the scan orientation from layer to layer to minimize residual stress build-up. Track width hatch spacing must be set so that adjacent beads overlap, and layer thickness settings must be less than the melt pool depth to produce a fully dense product. Sophisticated accessory equipment for melt pool imaging and real-time deposit height measurement has been developed for accurately monitoring the melt pool and deposit characteristics. It is possible to monitor the melt pool size, shape and temperature to maintain the desired pool characteristics. To control deposit thickness, travel speed can be dynamically changed based upon sensor feedback. Similarly to control solidification rate, and thus microstructure and properties, the melt pool size can be monitored and then controlled by dynamically changing laser power.

9.6 Typical Materials and Microstructure

BD processes aim to produce fully dense functional parts in metals and ceramics and are not meant for producing parts in plastic materials. Any metallic or ceramic powder or mixture thereof which is stable in a molten pool can be used for construction of parts. In general, metals with high reflectivities and thermal conductivities are difficult to process, such as gold and some alloys of aluminum and copper. Most other metals are quite straightforward to process, unless there is improper atmospheric preparation and bonding is inhibited by oxide formation. Generally, metallic materials that exhibit reasonably good weldability are easy to process.

Ceramics are more difficult to process, as fewer ceramics than metals can be heated to form a molten pool. Even in the event that a ceramic material can be melted to form a molten pool, cracking often occurs during cooling due to thermal shock. Thus, most ceramics that are processed using BD are processed as part of a ceramic or metal matrix composite.

For powder feedstock, the powder size typically ranges from approximately 20–150 μm. It is within this range that powder particles can be most easily fluidized and delivered using a flowing gas. Blended elemental powders can be used to produce an infinite number of alloy combinations or prealloyed powders can be used. Elemental powders can be delivered in precise amounts to the melt zone using separate feeders to generate various alloys and/or composite materials in-situ. When using elemental powders for generation of an alloy in-situ, the enthalpy of mixing plays an important role in determining the homogeneity of the deposited alloy. A negative enthalpy of mixing (heat release) promotes homogeneous mixing of constituent elements and, therefore, such alloy systems are quite suitable for processing using elemental powders.

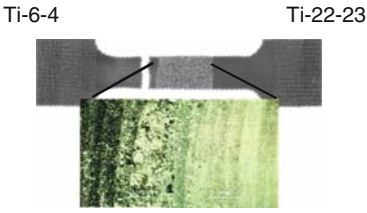

Fig. 9.10 Smooth transition between a 100% Ti-6-4- and 100% Ti-22-23 alloy in the gage section of a tensile bar. The transition region is shown at higher magnification (courtesy Optomec)

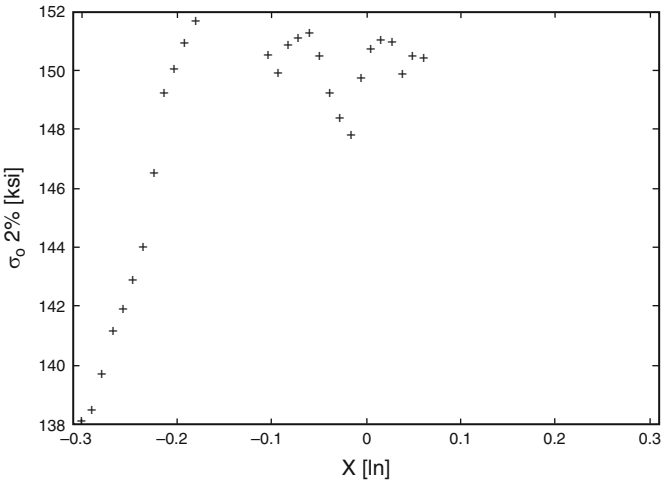

Fig. 9.11 Yield strength at various locations along the tensile bar from Fig. 9.10 representing the mechanical properties for different combinations of Ti-6-4 and Ti-22-23 (courtesy Optomec)

The fruitfulness of creating multi-material or gradient material combinations to investigate material properties quickly is illustrated in Figs. 9.10 and 9.11. Figure 9.10 illustrates a tensile bar made with a smooth 1D transition between Ti-6-4 and Ti-22-23, where Fig. 9.11 illustrates the yield strength of various combinations of these alloys. Using optical methods, localized stress and strain fields can be calculated during a tensile test and correlated back to the alloy combination for that location. Using this methodology, the properties of a wide range of alloy combinations can be investigated in a single experiment. Creating larger samples with 2D transitions of alloys (alloy transitions both longitudinally and transversely to the test axis using 3 or 4 powder feeders) can enable even greater numbers of alloy combinations to be investigated simultaneously.

Beam deposition processes can involve extremely high solidification cooling rates, from 10^3 to as high as $10^{5\circ}$C/s. This can lead to several microstructural advantages, including: (a) suppression of diffusion controlled solid-state phase transformations; (b) formation of supersaturated solutions and nonequilibrium phases; (c) formation of extremely fine microstructures with dramatically reduced elemental segregation; and (d) formation of very fine secondary phase particles (inclusions, carbides, etc.). Parts produced using BD experience a complex thermal history in a manner very similar to multi-pass weld deposits. Changes in cooling rate during part construction can occur due to heat build-up, especially in thin-wall sections. Also, energy introduced during deposition of subsequent layers can reheat previously deposited material, changing the microstructure of previously deposited layers. The thermal history, including peak temperatures, time at peak temperature and cooling rates, can be different at each point in a part, leading to phase transformations and a variety of microstructures within a single component.

As shown in Figs. 9.2, 9.3 and 9.10, parts made using BD typically exhibit a layered microstructure with an extremely fine solidification substructure. The interface region generally shows no visible porosity and a thin heat-affected zone (HAZ), as can be seen, for example, on the microstructure at the interface region of

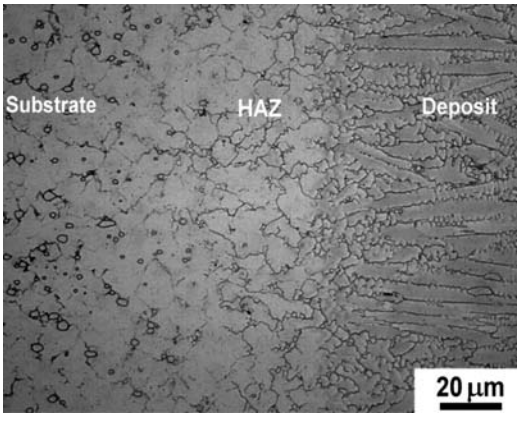

Fig. 9.12 CoCrMo LENS deposit on a wrought CoCrMo substrate of the same composition (deposit occurred from the right of the picture)

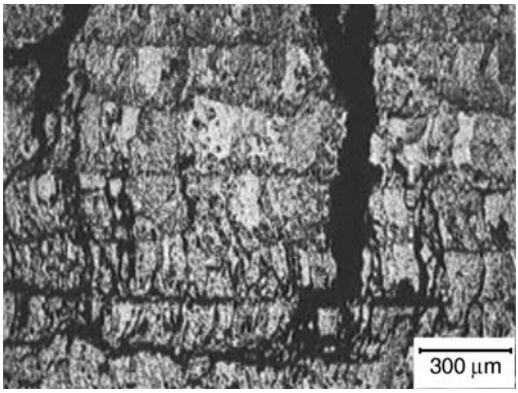

Fig. 9.13 Cracks in a TiC LENS deposit due to residual stresses [4]. (SCRIPTA MATERIALIA by Weiping Liu, and J. N. DuPont. Copyright 2003 by Elsevier Science & Technology Journals. Reproduced with permission of Elsevier Science & Technology Journals in the format Textbook via Copyright Clearance Center.)

a LENS deposited medical-grade CoCrMo alloy onto a CoCrMo wrought substrate of the same composition (Fig. 9.12). Some materials exhibit pronounced columnar grain structures aligned in the laser scan direction, while some materials exhibit fine equiaxed structures. The deposited material generally shows no visible porosity, although gas evolution during melting due to excess moisture in the powder or from entrapped gases in gas-atomized powders can cause pores in the deposit. Parts generally show excellent layer-to-layer bonding, although lack-of-fusion defects can form at layer interfaces when the process parameters are not properly optimized.

Residual stresses are generated as a result of solidification, which can lead to cracking during or after part construction. For example, LENS deposited TiC ceramic structures are prone to cracking as a result of residual stresses (Fig. 9.13). Residual stresses pose a significant problem when dealing with metallurgically incompatible dissimilar material combinations.

Formation of brittle intermetallic phases formed at the interface of dissimilar materials in combination with residual stresses can also lead to cracking. This can be overcome by suppressing the formation of the intermetallics using appropriate processing parameters or by the use of a suitable interlayer. For instance, in several research projects at Utah State University, it has been demonstrated that it is possible to suppress the formation of brittle intermetallics when depositing Ti on CoCrMo by placing the focal plane above the CoCrMo substrate during deposition of the first layer, and depositing a thin coating of Ti using a low laser power and rapid scan rate. Subsequent layers are likewise deposited using relatively thin deposits at high scan rates and low laser power to avoid reheating of the Ti/CoCrMo interface. If excess heat is introduced either during the deposition of subsequent layers or in subsequent heat treatment, the equilibrium intermetallics will form and cracking and delamination occurs. In other work, the same research group has successfully deposited CoCrMo on a porous Ta substrate when employing Zr as an interlayer material, a combination that is otherwise prone to cracking and delamination.

It is common for laser deposited parts to exhibit superior yield and tensile strengths because of their fine grain structure. Ductility of BD parts, however, is generally considered to be inferior to wrought or cast equivalents. Layer orientation can have a great influence on % elongation, with the worst being the z-direction. However, in many alloys ductility can be recovered and anisotropy minimized by heat treatment – without significant loss of strength in most cases.

9.7 Processing–Structure–Properties Relationships

Parts produced in beam deposition processes exhibit cast microstructures. Processing conditions influence the solidification microstructure in ways that can be predicted in part by rapid solidification theory. For a specific material, solidification microstructure essentially depends on the local solidification conditions, specifically the solidification rate and temperature gradient at the solid/liquid interface. By calculating the solidification rate and thermal gradient, the microstructure can be predicted based upon calibrated "solidification maps" from the literature.

To better understand solidification microstructures in beam deposition processes, Beuth and Klingbeil [5] have developed procedures for calculating thermal gradients, G, and solidification rates, R, analytically and numerically. These calculated G and R values can then be plotted on solidification maps to determine the types of microstructures which can be achieved with different beam deposition equipment, process parameters, and material combinations. Solutions for both thin-walls [5] and bulky deposits [6] have been described. For brevity's sake, the latter work by Bontha et al. [6] based upon the 3D Rosenthal solution for a moving point heat source on an infinite substrate will be introduced here (Fig. 9.14). This 3D Rosenthal solution also has application to PBF techniques.

In this simplified model, material deposition is ignored. The model considers only heat conduction within the melt pool and substrate due to a traveling heat source moving at velocity, V. The fraction of impinging energy absorbed is

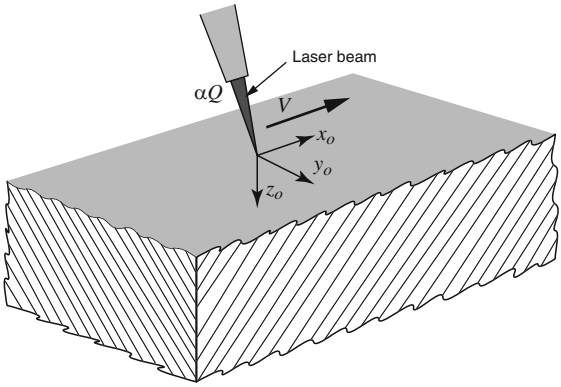

Fig. 9.14 3D Rosenthal geometry considered

αQ, which is a simplification of the physically complex temperature-dependent absorption of the beam by regions of the melt pool and solid, absorption of energy by powder in flight, and other factors. Thus a single parameter, α, represents the fraction of impinging beam energy power absorbed.

It is assumed the beam moves only in the x direction, and thus the beam's relative coordinates (x_0, y_0, z_0) from Fig. 9.14 are related to the fixed coordinates (x, y, z) at any time t as (x_0, y_0, z_0) = ($x-Vt$, y, z).

With the above conditions, the Rosenthal solution for temperature T at time t for any location in an infinite half-space can be expressed in dimensionless form as:

$$\bar{T} = \frac{e^{-\left(\bar{x}_0+\sqrt{\bar{x}_0^2+\bar{y}_0^2+\bar{z}_0^2}\right)}}{2\sqrt{\bar{x}_0^2+\bar{y}_0^2+\bar{z}_0^2}} \tag{9.1}$$

where

$$\begin{aligned} \bar{T} &= \frac{T-T_0}{(\alpha Q/\ \pi k)(\rho c V/2k)}, \\ \bar{x}_0 &= \frac{x_0}{(2k/\rho c V)}\ \bar{y}_0 = \frac{y_0}{(2k/\rho c V)} \text{ and } \bar{z}_0 = \frac{z_0}{(2k/\rho c V)}. \end{aligned} \tag{9.2}$$

In these equations, T_0 is the initial temperature, and ρ, c and k are density, specific heat and thermal conductivity of the substrate respectively. The thermophysical properties are assumed to be temperature independent, and are often selected at the melting temperature, as cooling rate and thermal gradient at the solid/liquid interface is of greatest interest.

The parameters of interest are solidification cooling rate and thermal gradient. The dimensionless expression for cooling rate becomes:

$$\begin{aligned} \frac{\partial \bar{T}}{\partial \bar{t}} = \frac{1}{2} & \frac{e^{-\left((\bar{x}-\bar{t})+\sqrt{(\bar{x}-\bar{t})^2+\bar{y}_0^2+\bar{z}_0^2}\right)}}{\sqrt{(\bar{x}-\bar{t})^2+\bar{y}_0^2+\bar{z}_0^2}} \\ & \times \left\{ 1 + \frac{(\bar{x}-\bar{t})}{\left(\sqrt{(\bar{x}-\bar{t})^2+\bar{y}_0^2+\bar{z}_0^2}\right)} + \frac{(\bar{x}-\bar{t})}{\left((\bar{x}-\bar{t})^2+\bar{y}_0^2+\bar{z}_0^2\right)} \right\}. \end{aligned} \tag{9.3}$$

where the dimensionless x coordinate is related to the dimensionless x_0 by $\bar{x} = \bar{x}_0 + \bar{t}$ where $\bar{t} = (t/(2k/\rho c V^2))$ and the dimensionless cooling rate is related to the actual cooling rate by:

$$\frac{\partial \bar{T}}{\partial \bar{t}} = \left(\frac{2k}{\rho c V}\right)^2 \left(\frac{\pi k}{\alpha Q V}\right) \frac{\partial T}{\partial t}. \tag{9.4}$$

The dimensionless thermal gradient is obtained by differentiating (9.1) with respect to the dimensionless spatial coordinates, giving

$$\left|\overline{\nabla T}\right| = \sqrt{\left(\frac{\partial \bar{T}}{\partial \bar{x}_0}\right)^2 + \left(\frac{\partial \bar{T}}{\partial \bar{y}_0}\right)^2 + \left(\frac{\partial \bar{T}}{\partial \bar{z}_0}\right)}, \tag{9.5}$$

where

$$\frac{\partial \bar{T}}{\partial \bar{x}_0} = -\frac{1}{2}\frac{e^{-\left(\bar{x}_0+\sqrt{\bar{x}_0^2+\bar{y}_0^2+\bar{z}_0^2}\right)}}{\sqrt{\bar{x}_0^2+\bar{y}_0^2+\bar{z}_0^2}} \times \left\{1+\frac{\bar{x}_0}{\left(\sqrt{\bar{x}_0^2+\bar{y}_0^2+\bar{z}_0^2}\right)}+\frac{\bar{x}_0}{\left(\bar{x}_0^2+\bar{y}_0^2+\bar{z}_0^2\right)}\right\}, \tag{9.6}$$

$$\frac{\partial \bar{T}}{\partial \bar{y}_0} = -\frac{1}{2}\frac{\bar{y}_0 e^{-\left(\bar{x}_0+\sqrt{\bar{x}_0^2+\bar{y}_0^2+\bar{z}_0^2}\right)}}{\left(\bar{x}_0^2+\bar{y}_0^2+\bar{z}_0^2\right)}\left\{1+\frac{1}{\left(\sqrt{\bar{x}_0^2+\bar{y}_0^2+\bar{z}_0^2}\right)}\right\}, \tag{9.7}$$

and

$$\frac{\partial \bar{T}}{\partial \bar{z}_0} = -\frac{1}{2}\frac{\bar{z}_0 e^{-\left(\bar{x}_0+\sqrt{\bar{x}_0^2+\bar{y}_0^2+\bar{z}_0^2}\right)}}{\left(\bar{x}_0^2+\bar{y}_0^2+\bar{z}_0^2\right)}\left\{1+\frac{1}{\left(\sqrt{\bar{x}_0^2+\bar{y}_0^2+\bar{z}_0^2}\right)}\right\}. \tag{9.8}$$

As defined above, the relationship between the dimensionless thermal gradient $\left|\overline{\nabla T}\right|$ and the actual thermal gradient $|\nabla T|$ is given by

$$\left|\overline{\nabla T}\right| = \left(\frac{2k}{\rho c V}\right)^2\left(\frac{\pi k}{\alpha Q}\right)|\nabla T|. \tag{9.9}$$

Using this formulation, temperature, cooling rates and thermal gradients can be solved for any location (x,y,z) and time (t).

For microstructure prediction purposes, solidification characteristics are of interest; and thus we need to know the cooling rate and thermal gradients at the boundary of the melt pool. The roots of (9.1) can be solved numerically for temperature T equal to melting temperature T_m to find the dimensions of the melt pool. Similarly to (9.2) for normalized temperature, normalized melting temperature can be represented by:

$$\bar{T}_\mathrm{m} = \frac{T_\mathrm{m} - T_0}{(\alpha Q/\ \pi k)(\rho c V/2k)}. \tag{9.10}$$

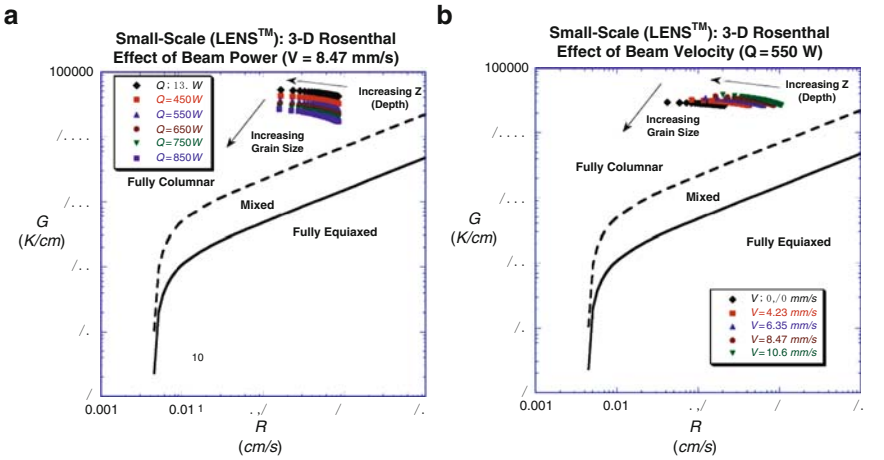

Fig. 9.15 Process maps showing microstructures predicted by the 3D Rosenthal solution for a lower-powered (LENS-like) beam deposition system for Ti–6Al–4V (MATERIALS SCIENCE & ENGINEERING. A. STRUCTURAL MATERIALS : PROPERTIES, MICROSTRUCTURE AND PROCESSING by Srikanth Bontha, Nathan W. Klingbeil, Pamela A. Kobryn and Hamish L. Fraser. Copyright 2009 by Elsevier Science & Technology Journals. Reproduced with permission of Elsevier Science & Technology Journals in the format Textbook via Copyright Clearance Center.)

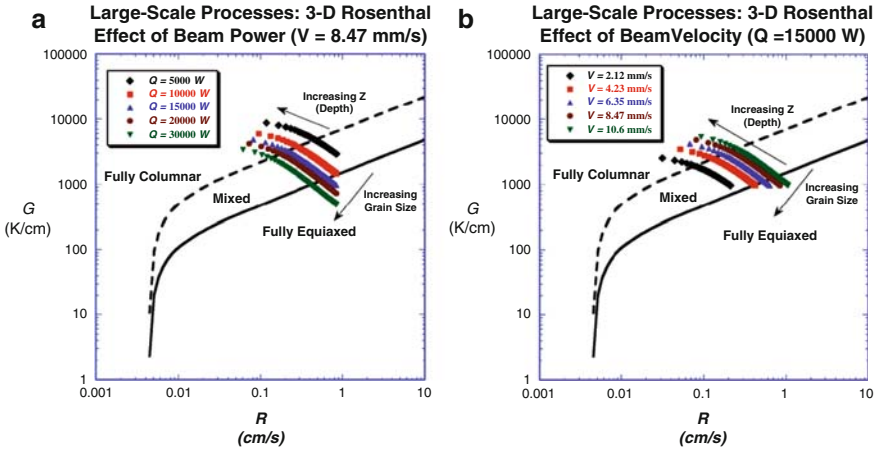

Fig. 9.16 Process maps showing microstructures predicted by the 3D Rosenthal solution for a higher-powered (AeroMet-like) beam deposition system for Ti–6Al–4V(MATERIALS SCIENCE & ENGINEERING. A. STRUCTURAL MATERIALS : PROPERTIES, MICROSTRUCTURE AND PROCESSING by Srikanth Bontha, Nathan W. Klingbeil, Pamela A. Kobryn and Hamish L. Fraser. Copyright 2009 by Elsevier Science & Technology Journals. Reproduced with permission of Elsevier Science & Technology Journals in the format Textbook via Copyright Clearance Center.)

Given cooling rate $\frac{\partial T}{\partial t}$ from (9.4) and thermal gradient, G, defined as $G = |\nabla T|$, we can define the solidification velocity, R, as

$$R = \frac{1}{G}\frac{\partial T}{\partial t}. \tag{9.11}$$

We can now solve these sets of equations for specific process parameters (i.e., laser power, velocity, material properties, etc.) for a machine/material combination of interest. After this derivation, Bontha et al. [6] used this analytical model to demonstrate the difference between solidification microstructures which can be achieved using a small scale beam deposition process with a lower-powered laser beam, such as utilized in a LENS machine, compared to a high-powered laser beam system, such as practiced by AeroMet for Ti–6Al–4V. Assumptions included the thermophysical properties of Ti–6Al–4V at T_m = 1,654°C, a room temperature initial substrate temperature T_0 = 25°C, fraction of energy absorbed α = 35, laser power from 350 to 850 W and beam velocity ranging from 2.12 to 10.6 mm/s. For the high-powered beam system, a laser power range from 5 to 30 kW was selected. A set of graphs representing microstructures with low-powered systems is shown in Fig. 9.15. Microstructures from high-powered systems are shown in Fig. 9.16 for comparison.

As can be seen from Fig. 9.15, lower-powered beam deposition systems cannot create mixed or equiaxed Ti–6Al–4V microstructures, as the lower overall heat input means that there are very large thermal gradients. For higher-powered beam deposition systems, it is possible to create dendritic, mixed or fully equiaxed microstructures depending upon the process parameter combinations used. As a result, without the need for extensive experimentation, process maps such as these, when combined with appropriate modeling, can be used to predict the type of beam deposition system (specifically the scan rates and laser power) needed to achieve a desired microstructure type for a particular alloy.

9.8 BD Benefits and Drawbacks

BD processes are capable of producing fully-dense parts with highly controllable microstructural features. These processes can produce functionally graded components with composition variations in the X, Y and Z directions.

The main limitations of beam deposition processes are poor resolution and surface finish. An accuracy better than 0.25 mm and a surface roughness of less than 25 μm (arithmetic average) are difficult with many processes. Slower build speed is another limitation. Build times can be very long for these processes, with typical deposition rates as low as 25–40 g/h. To achieve better accuracies, small beam sizes and deposition rates are required. Conversely, to achieve rapid deposition rates, degradation of resolution and surface finish result. Changes in laser power and scan rate to achieve better accuracies or deposition rates may also affect

the microstructures of the deposited components, and thus finding an optimum deposition condition necessitates tradeoffs between build speed, accuracy and microstructure.

Examples of the unique capabilities of beam deposition include:

- BD offers the capability for unparalleled control of microstructure. The ability to change material composition and solidification rate by simply changing powder feeder mixtures and process parameters gives designers and researchers tremendous freedom. This design freedom is further explored in Chap. 11.
- BD is capable of producing directionally solidified and single crystal structures.
- BD can be utilized for effectively repairing and refurbishing defective and service damaged high-technology components such as turbine blades.
- BD processes are capable of producing in-situ generated composite and heterogeneous material parts. For example, Banerjee et al. [7] have successfully produced Ti–6Al–4V/TiB composite parts using the LENS process employing a blend of pure pre-alloyed Ti–6Al–4V and elemental B powders (98 wt% Ti–6Al–4V + 2 wt% B). The LENS deposited material exhibited a homogeneous refined dispersion of nano-scale TiB precipitates within the Ti–6Al–4V α/β matrix.
- BD can be used to deposit thin layers of dense, corrosion resistant and wear resistant metals on components to improve their performance and lifetime. One example includes deposition of dense Ti/TiC coatings as bearing surfaces on Ti biomedical implants, as illustrated in Fig. 9.2.

When contrasted with other AM processes, BD processes cannot produce as complex of structures as, for instance, powder bed fusion processes. This is due to the need for support structures or multi-axis deposition for certain complex geometries.

Post-processing of parts made using BD typically involves removal of support structures or the substrate, if the substrate is not intended to be a part of the final component. Finish machining operations because of relatively poor part accuracy and surface finish are commonly needed. Stress relief heat treatment may be required to relieve residual stresses. In addition, depending upon the material, heat treatment may be necessary to produce the desired microstructure(s). For instance, parts constructed in age-hardenable materials will require either a direct aging treatment or solution treatment followed by an aging treatment to achieve precipitation of strengthening phases.

BD processes are uniquely suited amongst AM process for repair and feature addition. As this AM process is formulated around deposition, there is no need to deposit on a featureless plate or substrate. Instead, BD is often most successful when used to add value to other components by repairing features, adding new features to an existing component and/or coating a component with material which is optimized for the service conditions of that component in a particular location.

As a result of the combined strengths of BD processes, practitioners of BD primarily fall into one of several categories. First, BD has been highly utilized by research organizations interested in the development of new material alloys and the

application of new or advanced materials to new industries. Second, BD has found great success in facilities that focus on repair, overhaul, and modernization of metallic structures. Third, BD is useful for adding features and/or material to existing structures to improve their performance characteristics. In this third category, BD can be used to improve the life of injection molding or die casting dies by depositing wear-resistant alloys in high-wear locations; it is being actively researched by multiple biomedical companies for improving the characteristics of biomedical implants; and it is used to extend the wear characteristics of everything from drive shafts to motorcycle engine components.

9.9 Exercises

1. Discuss 3 characteristics where BD is similar to extrusion-based processes and 3 characteristics where BD is different than extrusion-based processes.
2. Read reference [4] related to thin-wall structures made using BD. What are the main differences between modeling thin-wall and bulky structures? What ramifications does this have for processing?
3. Why is solidification rate considered the key characteristic to control in BD processing?
4. From the literature, determine how solidification rate is monitored. From this information, describe an effective, simple closed-loop control methodology for solidification rate.
5. Why are BD processes particularly suitable for repair?

References

1. Keicher DM, Miller WD (1998) Metal Powder Report 53:26
2. Lewis GK et al (1994) Directed light fabrication. In: Proceedings of the ICALEO ’94. Laser Institute of America, Orlando, FL, p 17
3. House MA et al (1996) Rapid laser forming of titanium near shape articles: LaserCast. In: Proceedings of the solid freeform fabrication symposium, Austin, TX, p 239
4. Liu W, DuPont JN (2003) Fabrication of functionally graded TiC/Ti composites by Laser Engineered Net Shaping. Scr Mater 48:1337
5. Beuth J, Klingbeil N (2001) The role of process variables in laser based direct metal solid freeform fabrication. J Met 9:36–39
6. Bontha S, Klingbeil NW, Kobryn PA, Fraser HL (2009) Effects of process variables and size-scale on solidification microstructure in beam-based fabrication of bulky 3D structures. Materials Science & Engineering. A. Structural Materials: Properties, Microstructure And Processing Vol. 513–514, pp 311–318, July 15
7. Banerjee R et al (2003) Direct laser deposition of in situ Ti–6Al–/4 V–/TiB composites. Mater Sci Eng A A358:343